JOURNAL OF PROPULSION AND POWER
Vol. 16, No. 2, March–April 2000

Numerical Investigation of Twin-Nozzle Rocket Plume Phenomenology

Houshang B. Ebrahimi*
Sverdrup Technology, Inc., Arnold Air Force Base, Tennessee 37389-6001
Jay Levine†
U.S. Air Force Research Laboratory, Edwards Air Force Base, California 93524
and
Alan Kawasaki‡
Sparta, Inc., Edwards Air Force Base, California 93524

The generalized implicit flow solver (GIFS) computer program has been modified and applied for the analysis of three-dimensional reacting two-phase flow simulation problems. The intent of the original GIFS development effort was to provide the joint Army, Navy, NASA, Air Force community with a standard computational methodology to simulate the complete flowfield of propulsion systems including multiple nozzle/plume flowfield phenomena and other three-dimensional effects. The Van Leer flux splitting option has been successfully implemented into the existing GIFS model and provides a more robust solution scheme, making application of the model more reasonable for engineering applications. Significant results of several twin-nozzle/plume simulations using the GIFS code are reported. Eight simulations of Titan II plume flowfields have been completed to assess the effects of three dimensionality, turbulent viscosity, afterburning, near-field shock structure, finite rate kinetic chemistry, internozzle geometric spacing, nozzle exit plane profile, and missile body on the subsequent plume exhaust flowfield. The results of these calculations indicate that the viscous stress model; kinetic chemistry, particularly at lower altitudes; and nozzle exit profile may be important parameters that should be considered in the analyses and the interpretation of radar signature calculations. Three dimensionality is also an important influence, which can substantially influence the interpretation of the results. If three-dimensional effects are oversimplified in the model, analyses of the spatial results can be misinterpreted and misapplied. In addition, the missile body effect and internozzle geometric spacing influence the expansion shock reflection location that can significantly affect the plume/plume impingement shock location, inviscid shock structure, and shear-layer growth.

Introduction

TO support propulsion testing and analysis requirements of the aerospace and exhaust plume communities, a need exists for a fluid dynamics model that solves the fully coupled, two-phase Navier–Stokes (NS) equations in multiple dimensions. Evaluation of solid-propellant rocket motor performance and rocket plume radiative transfer analyses requires a computer model that simulates complex three-dimensional, chemically reacting two-phase flow effects.[1] In the past few years, significant progress has been made in the areas of numerical rocket flow simulations and computational resources to the point that NS solutions are viable analysis tools. Although this type of full-NS method provides an accurate qualitative description of the basic features of the propulsion-generated flowfields, quantitative simulations for predicting fundamental parameters such as base pressure and heat transfer, gas static pressure, gas and particulate temperatures, and chemical composition in the flowfield domain have not been validated.

The flowfields generated by rocket propulsion systems are complex, with regions of strong inviscid/viscous interactions, freestream shear layers, nozzle wall and missile body boundary layers, external and internal shocks, separation regions, and plume/plume impingement and associated flow interactions for multiple nozzle designs, all with chemically reacting kinetics.[2] Coupling all of these phenomena simultaneously in a numerical simulation tool challenges the state of the art for computational fluid dynamics (CFD) models. To account for the significant phenomena affecting plume flow properties and the resulting radiative transfer implications, computationally efficient multidimensional computer models are required.

Recently, there has been increased emphasis on the application of existing CFD models, both in the commercial arena and government-developed computer programs, to simulate complex multidimensional plume phenomena. A large majority of the solutions obtained to date are based on the perfect gas (constant gamma) approximation, as fully reacting flows are considerably more complex and difficult to solve. Including the effects of chemistry in the solution produces a stiff set of equations that are numerically difficult to solve using conventional algorithms. In addition, the grid resolution requirements become more severe, and time-step issues arise when reacting chemistry is included in the NS model.

Conventional rocket exhaust flow computer models[3,4] employ Euler solutions for the inviscid plume core flow region. Overlaid onto the inviscid solution is an uncoupled, parabolic mixing methodology for the turbulent, chemically reacting, freestream air entrainment in the shear-layer region. These methods are generally not adequate for situations when the flow is not fully dominated by either inviscid core gasdynamics or the plume afterburning phenomena. Three-dimensional features produced by multiple nozzle propulsion systems and vehicle body/base interactions cannot be sufficiently treated through the use of these models. Inaccurate accounting of the three-dimensional upstream influences on the plume shear-layer development and the resulting plume structure is one of the primary issues preventing approximate models from accurately simulating the overall flowfield phenomena.[5]

The generalized implicit flow solver (GIFS) numerical algorithm provides a solution of the two- and three-dimensional Reynolds-averaged NS equations using the MacCormack implicit finite volume algorithm with Gauss–Seidel line relaxation.[6] Several two- and three-dimensional plume flowfield calculations have been

Received 8 December 1997; revision received 4 November 1998; accepted for publication 20 November 1998.

*Senior Research Engineer, Arnold Engineering Development Center.
†Chief, Aerophysics Branch.
‡Senior Propulsion Engineer.

completed for the plume near-field region using the original version of the GIFS model.[6] The GIFS model includes a frozen and a generalized finite rate kinetic chemistry model, a Lagrangian particle model for treating solid and liquid particulates, and a two-equation k-ε turbulence model, as well as laminar flows. These complex phenomena are required to accurately simulate the physics expected to contribute to the flowfield spatial distribution of gasdynamic, thermodynamic, and chemical properties. The Van Leer flux splitting option[7] has been successfully implemented into the original GIFS model and provides a more robust solution scheme for simulating propulsion flowfield phenomena.[8] Convergence characteristics, using the Van Leer scheme, are vastly improved, particularly in regions of high property gradients, where the solution stabilizes more rapidly, and thereby allows the use of larger Courant–Friedrichs–Lewy values.

The enhanced version of the GIFS model was applied in this study. A previous investigation[8] focused on the validation of the enhanced version of the GIFS model using an extensive database of laboratory measurements. The validation focused on the combustion, turbulence, and three-dimensional aspects of the model. Comparisons of the GIFS calculation results with the measurements were encouraging.

The near-field plume flowfield emanating from a multinozzle vehicle flying at high altitude is largely dominated by the processes taking place in the plumes' interaction region. Prior to the release of the GIFS model, simulations of multiple nozzle/plume flowfields were commonly treated by assuming a single equivalent nozzle configuration having equal mass, energy, and momentum of the multiple nozzle geometry. Further, as a simplifying assumption, uniform (one-dimensional) nozzle exit flow properties were used as the starting conditions for the plume calculation. The simplified model assumes that the details of the three-dimensional flow structure in the near-field region and the uniform start condition are unimportant, and that the flow processes affecting the plume shear-layer initialization (such as base separation and recirculation) will be dominated by the overall ambient flow entrainment effects. For analyses requiring spatial detail and accuracy, the level of agreement between computations based on the simplified single-equivalent nozzle methodology and simulations from multiple-nozzle propulsion systems has not been acceptable. The source of the disagreement is caused, at least in part, by an incorrect physical model of the phenomena dominating the observations, e.g., inadequate turbulence, incomplete chemical mechanisms, missing or inaccurate reaction rates, simplified initial start conditions, and three-dimensional geometry effects. The actual physical geometries are often oversimplified, and relevant details of the engine design and the resulting impact on the initial conditions and the downstream exhaust flow are frequently ignored.

The motivation for this study is to demonstrate the significance of three-dimensional effects as applied to multiple nozzle missile plumes to determine how these phenomena may be simplified and incorporated into engineering analysis models. The knowledge gained can be applied to promote improvements to engineering approaches and to explore methods to reduce the overall CPU resource requirements for three-dimensional computer simulations. While it is recognized that grid issues affect the solution integrity, grid refinement was not a part of this study.

Computations

The computational effort consisted of seven, three-dimensional twin-nozzle simulations and one two-dimensional axisymmetric calculation for the Titan II vehicle at flight conditions. In the first six cases, only the plume flowfield was computed; i.e., missile base effects were not considered. Also, in the first five cases, boundary-layer effects from inside the rocket nozzle were not considered. The starting boundary conditions at the nozzle exit plane were assumed to be uniform for these cases. In the sixth case, the plume flowfield was computed utilizing a two-dimensional, viscous radial profile starting conditions at the nozzle exit plane. The GIFS model was initiated at the nozzle exit plane using results obtained from the two-dimensional kinetic computer program.[9] The GIFS model was then applied to simulate the external plume flowfield. For all cases, the plume flowfield was simulated at an altitude of 47.6 km, and the vehicle Mach number was 5.7. The nozzle operated in a significantly underexpanded mode ($P_e \gg P_\infty$). In the first six cases, the resulting nozzle exit-to-freestream velocity ratio was ~5, and the chamber pressure to freestream pressure ratio was ~50,000:1.

Table 1 Parametric flowfield conditions

Case	Viscosity	Inlet profile	Chemistry	Nozzle spacing	Gas generator
1	Laminar	One-dimensional	Constant γ	Wide	No
2	Turbulent	One-dimensional	Constant γ	Wide	No
3	Turbulent	One-dimensional	Constant γ	Narrow	No
4	Turbulent	One-dimensional	Frozen	Narrow	No
5	Turbulent	One-dimensional	Finite rate	Narrow	No
6	Turbulent	Two-dimensional	Finite rate	Narrow	No
7	Turbulent	Two-dimensional	Finite rate	Narrow	Yes
8	Turbulent	Two-dimensional	Finite rate	Two-dimensional axisymmetric	No

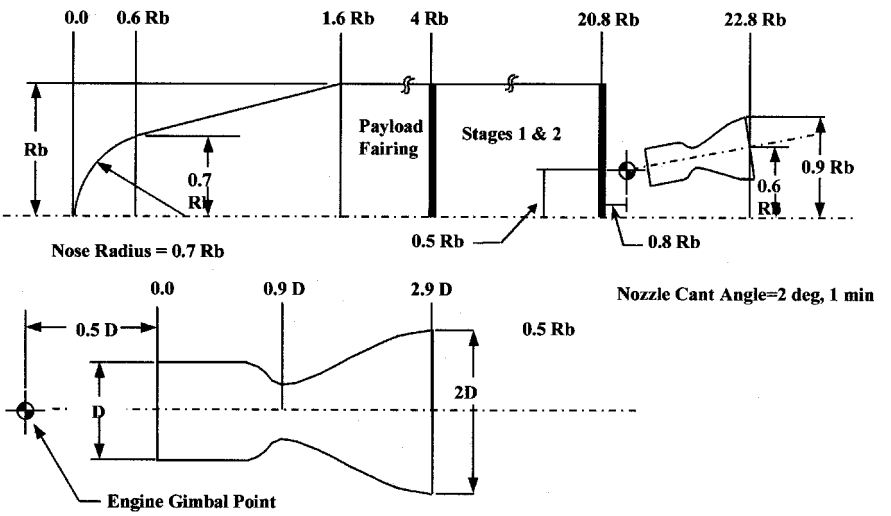

Fig. 1 Vehicle dimensions.

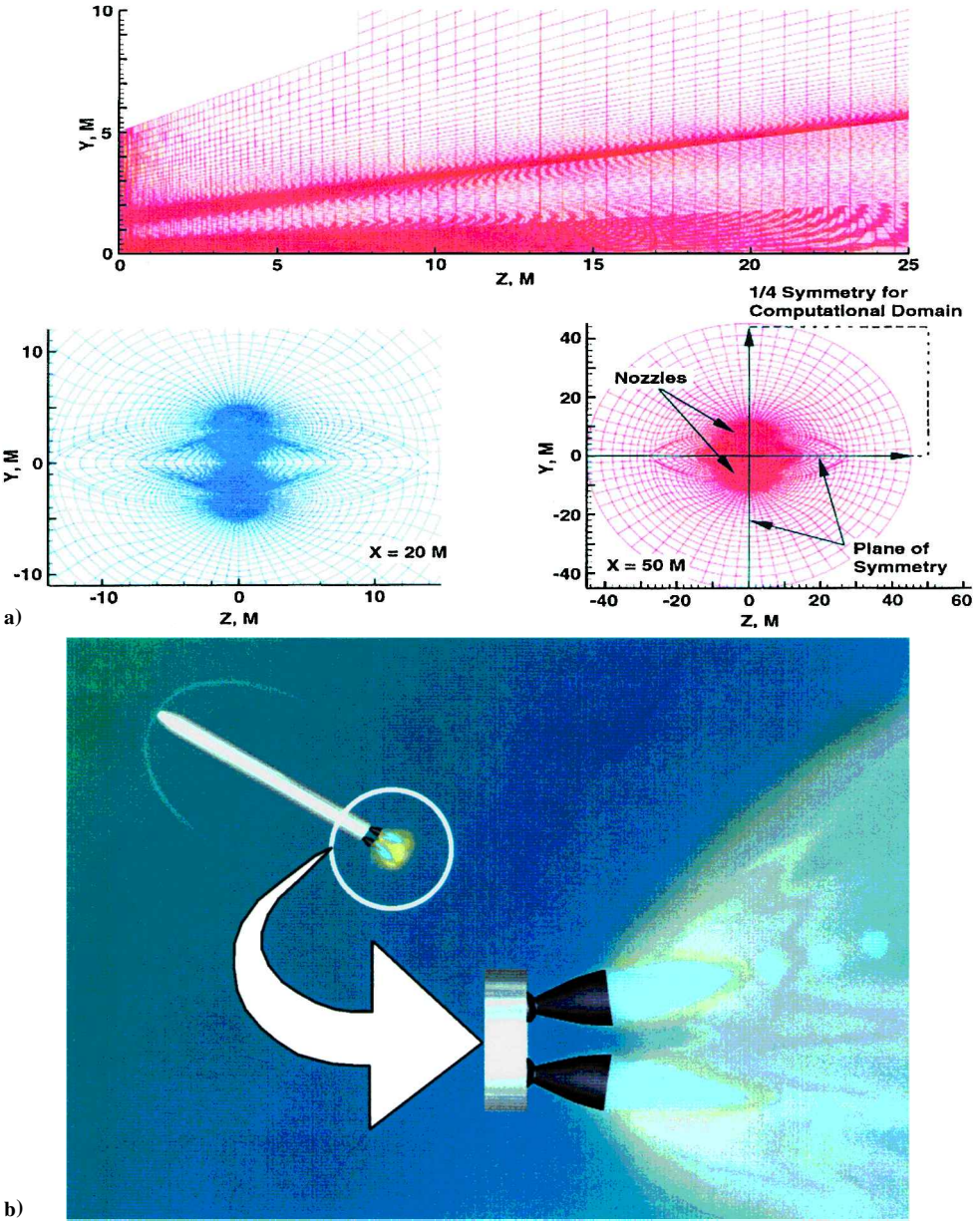

Fig. 2 Geometry representation of the computation domain. Schematic of the a) three-dimensional grid and the planes of symmetry and b) of the three-dimensional plume.

In the last three-dimensional case, a complete solution, including the external flow over the missile body, the base region, and the gas generator flow was included in this simulation. To provide a contrasting solution to the three-dimensional flowfield simulations, an axisymmetric approximation for the dual nozzle plumes was computed. In this case, the mass flow from the dual engine was matched by scaling up the single engine dimensions by the square root of 2. The parametric flowfield conditions and assumptions for all eight cases are summarized in Table 1.

The Titan II Space-Launched Vehicle propulsion system is propelled by two engines located on either side of a plane of symmetry passing through the vehicle centerline. Figure 1 is a schematic of the vehicle. The sea-level rated thrust derived from each engine is ~214,000 lbf. Roll, pitch, and yaw control are provided by gimballing of the engine ±5 deg from the engine neutral position (2-deg cant angle away from the vehicle centerline for both nozzles). The 2-deg cant angle was included in the three-dimensional simulations.[10] Both nozzles are identical in geometry and operating conditions.

The thrust chamber assemblies and nozzle skirt are regeneratively cooled. In addition, injector spray patterns intentionally direct a

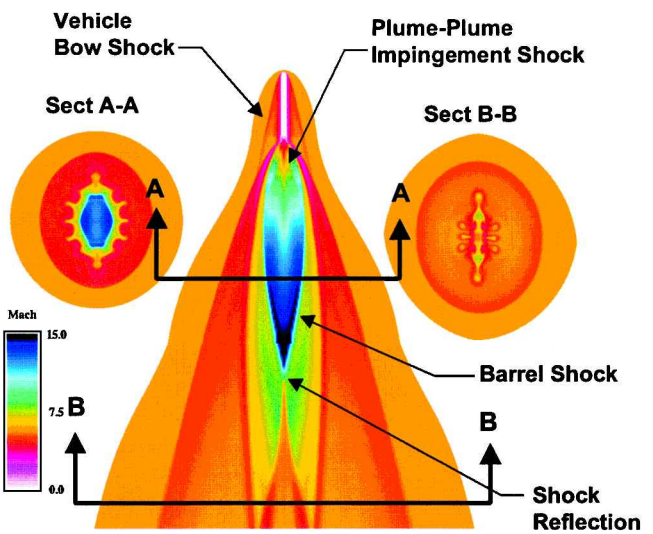

Fig. 3 Mach contours (three-dimensional calculation).

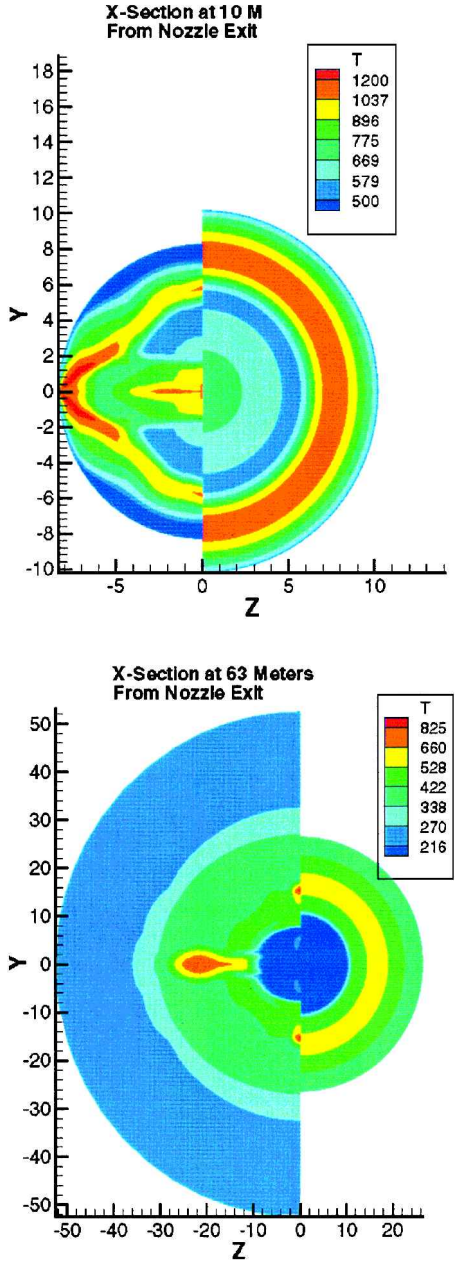

Fig. 4 Static temperature cross-sectional comparisons, three-dimensional plume vs single equivalent nozzle.

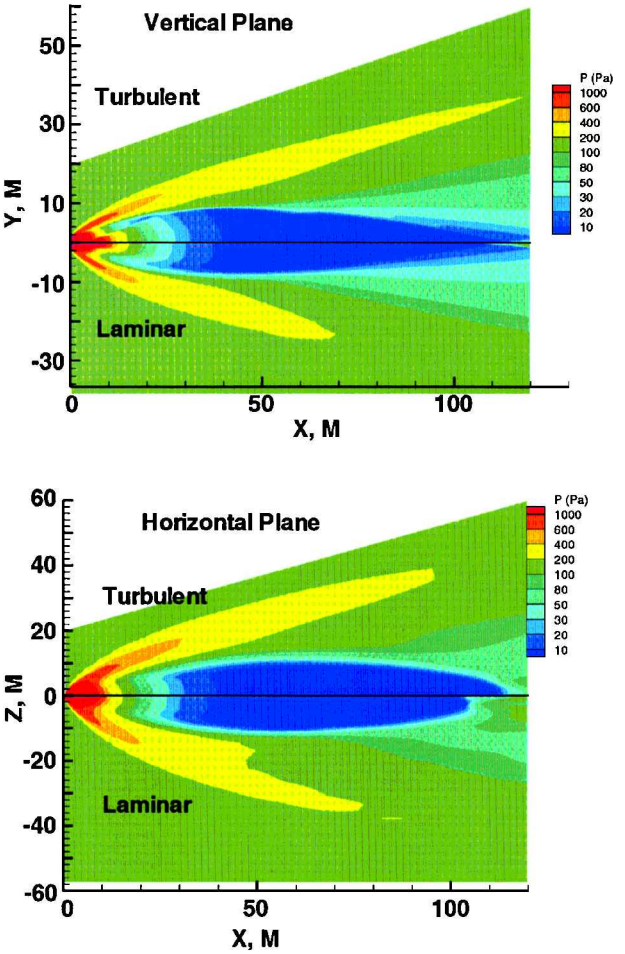

Fig. 5 Laminar and turbulent pressure comparisons.

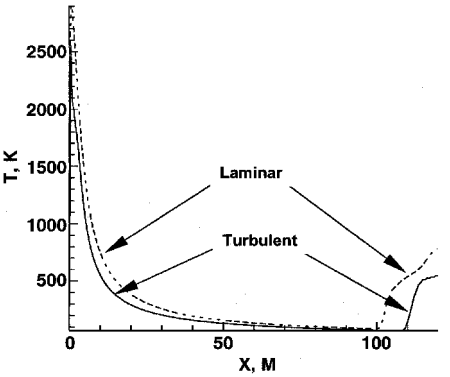

Fig. 6 Static temperature comparison along centerline.

fuel-rich layer adjacent to the chamber walls to reduce the wall heat loads. The engine fuel is AEROZINE-50, a $\frac{50}{50}$ blend of hydrazine (N_2H_4) and unsymmetrical dimethylhydrazine ($C_2H_8N_2$), and the oxidizer is N_2O_4. Power to drive the turbopumps is derived from two gas generators, which represent ~1.5% of the overall propellant expended by both engines. These gas generators are intentionally operated at fuel-rich conditions to minimize heat loads on the turbine blades.

To limit the number of grid points and CPU run time, quarter symmetry assumptions were made for the computational domain plane. Zero angle of attack and dual plume exhaust were two additional constraints imposed for these simulations. A total of 600,000 grid points were utilized in the computational domain for the first six cases, 4 million grid points for the last three-dimensional case, and 200,000 grid points for the axisymmetric case. It should be noted that for the three characteristic cases, i.e., three-dimensional flying plume, three-dimensional plume with body, and the axisymmetric plume with body, the grid resolution was not consistently set. The 600,000 node grid was quite coarse for the three-dimensional flying plume cases, but for the purposes of making qualitative comparisons between similar cases (cases 1–6), the basic features from these solutions appeared to be adequately resolved. In the last two cases, grid resolution was sufficiently refined. The exhaust plume portion of the computational domain is shown in Fig. 2a with the orientation indicated by the axes. A schematic of the three-dimensional plume configuration is shown in Fig. 2b.

External airflow conditions, engine nozzle exit conditions, throat conditions, and gas generator conditions for the Titan test cases are presented next:

1) Ambient conditions at 47.6 km: $T = 269$ K, $V = 1877.6$ m/s, $C_p/C_v = 1.4$, $\rho = 1.388 \times 10^{-3}$ kg/m^3, $P = 108$ Pa, and Mach = 5.7. Species concentrations (mass fraction): $N_2 = 0.77$ and $O_2 = 0.23$.

2) Jet conditions (one dimensional): $T = 1920$ K, $V = 2776.6$ m/s, $P = 92{,}800$ Pa, $\rho = 1.68 \times 10^{-1}$ kg/m^3, and Mach = 3.0. Species concentrations (mass fraction): CO = 0.039, $N_2 = 0.414$,

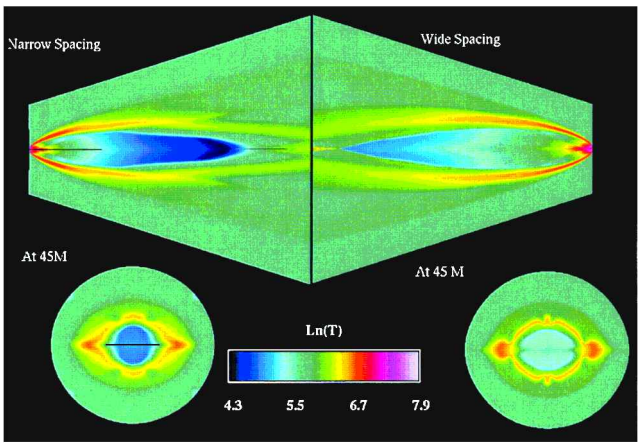

Fig. 7 Perfect gas comparisons of temperature contours illustrating nozzle spacing effects.

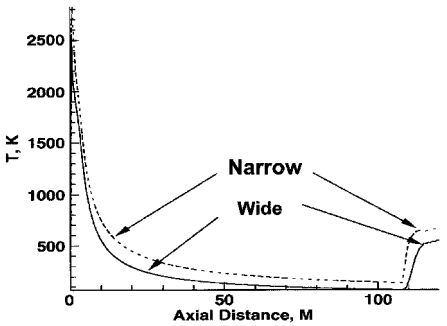

Fig. 8 Temperatures along vehicle centerline comparing nozzle spacing effects.

$H_2 = 3.13e{-}3$, $CO_2 = 0.1811$, $NO = 0.0109$, $H = 1.24e{-}4$, $H_2O = 0.3496$, $OH = 2.139e{-}3$, $O_2 = 0.0$, and $O = 0.0$.

3) Gas generator conditions: $M = 1.01$, $T = 899$ K, $P = 85{,}488.9$ Pa, $CO = 0.04$, $CO_2 = 0.004$, $CH_4 = 0.135$, $H_2 = 0.035$, $H_2O = 0.034$, $NH_3 = 0.253$, and $C = 0.038$. (T, P, and ρ are static conditions.)

The finite rate chemical kinetic simulations used a chemical reaction model consisting of 11 species and 210 reactions for carbon-, hydrogen-, oxygen-, and nitrogen-based propellant systems.[9] The rate-controlled reactions included the recombination and dissociation of nine species: CO, CO_2, N_2, H_2, H, H_2O, OH, O_2, and O. Two additional compounds, methane (CH_4) and ammonia (NH_3), were included as part of the overall mixture, for completeness. However, neither methane nor ammonia was allowed to react within the flow exhaust. Because these species were in small concentrations, it was assumed that the decomposition of these species would not significantly contribute to the heat release nor alter the mixture sufficiently to impact the overall simulation.

The k-ε turbulence model[11] was applied for viscous stress approximation. The computation was performed on a single processor SGI Power Challenge R8000. For the first six cases, the calculations executed for ~11,000 iterations. Case 7, the three-dimensional calculation including the missile body/base and gas generator, was the most stressing case. This solution required approximately three months of CPU time to converge. In contrast, the axisymmetric case required 4 days to converge.

Seven three-dimensional numerical calculations of the twin-nozzle configuration were obtained at Mach 5.7 for different combinations of flow assumptions and approximations in an attempt to isolate individual influences and effects. Cases 1 and 2 compare laminar flow and turbulent viscous stress models, respectively, and were computed assuming a perfect gas equation of state. Case 3 is a turbulent, constant-gamma approximation with an internozzle geometric spacing that differed from cases 1 and 2. Cases 4 and 5 contrast frozen- and finite rate chemistry, respectively. Cases 1–5 all assume uniform nozzle exit properties as the GIFS start-line conditions. Case 6 is a chemically reacting plume exhaust using

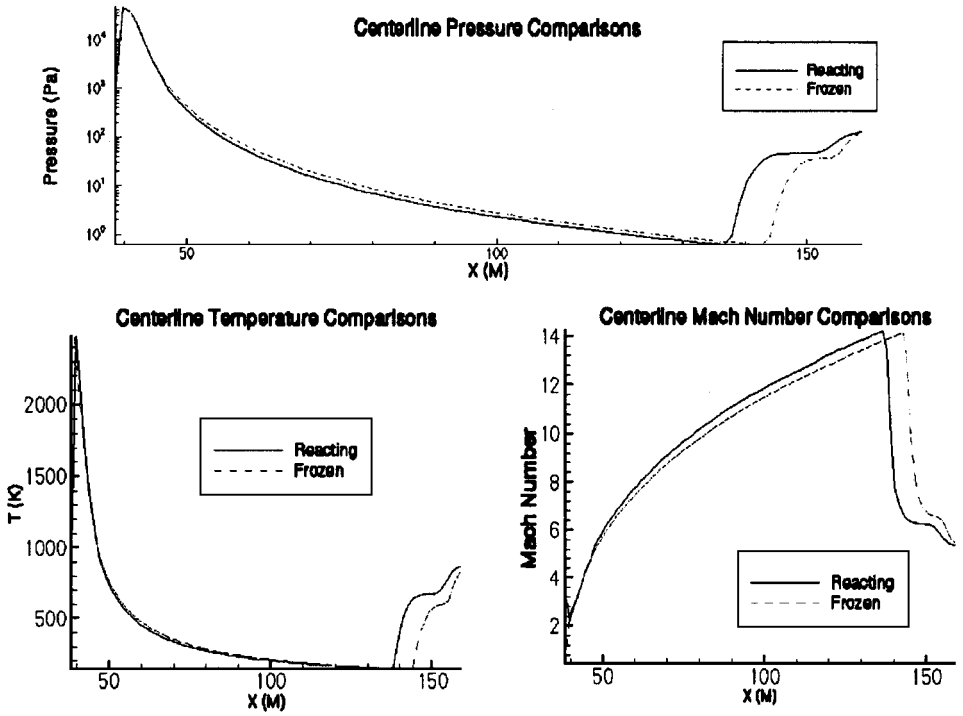

Fig. 9 Pressure, temperature, and Mach number comparison of reacting vs frozen.

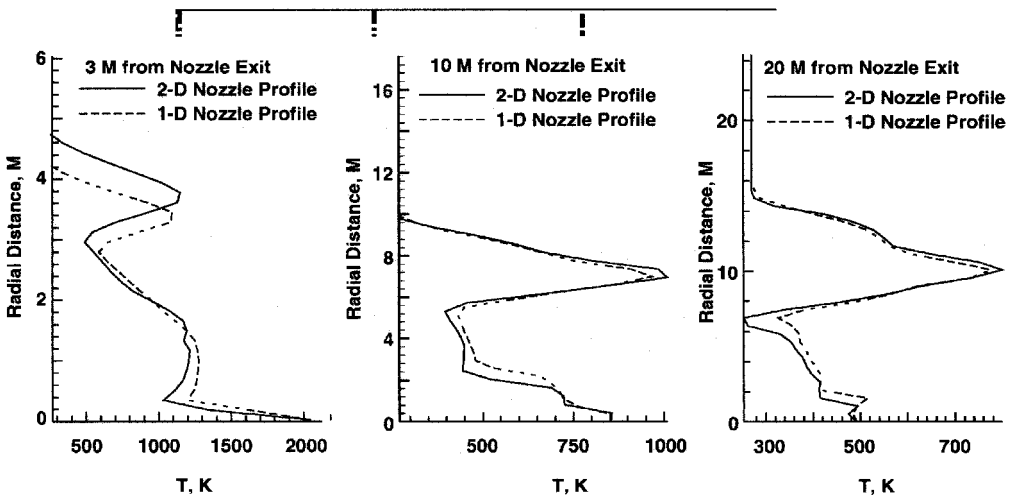

Fig. 10 Y–Z temperature profile at X = 3, 10, and 20 m.

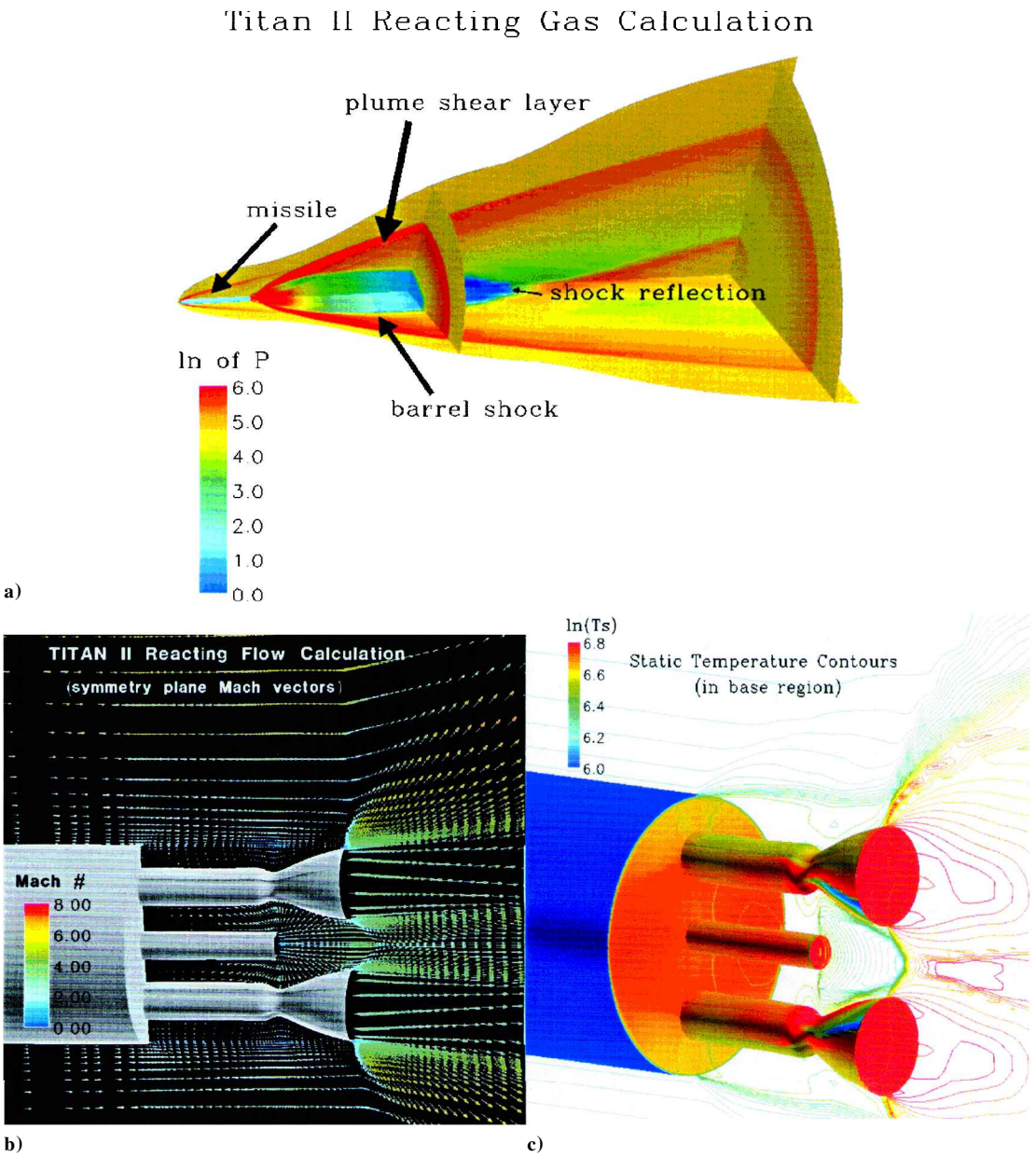

Fig. 11 Nose-to-tail three-dimensional calculations: a) pressure contours, b) Mach vectors, and c) isotherms.

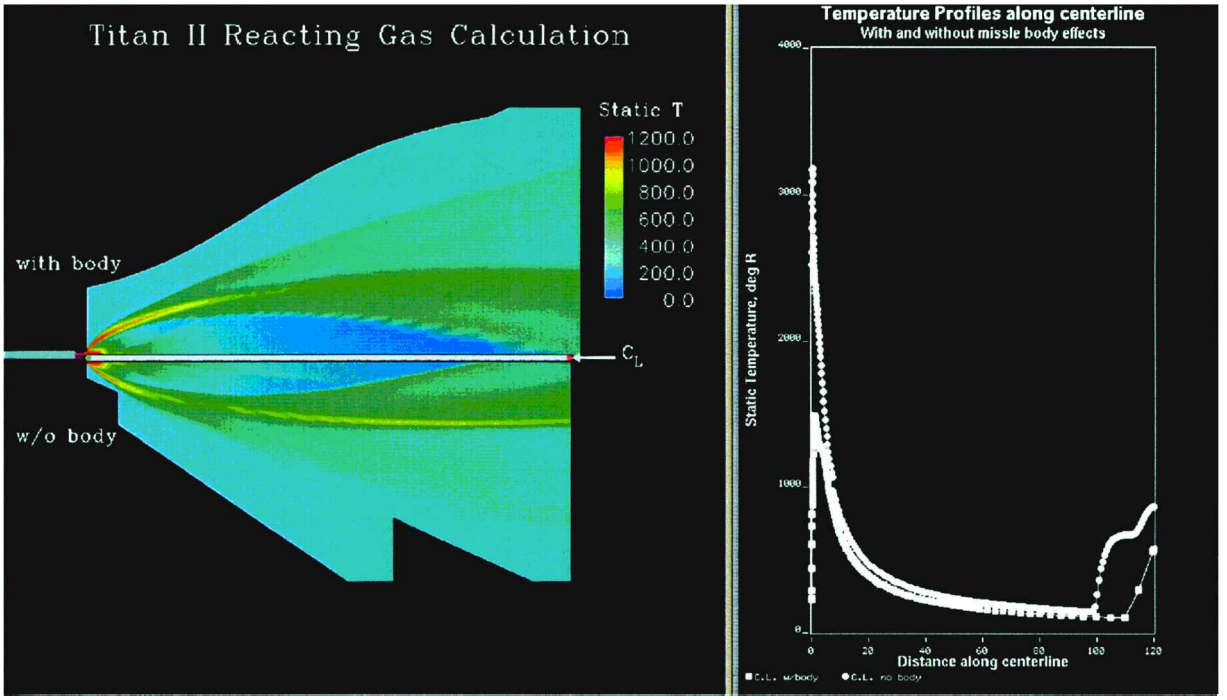

Fig. 12 Static temperature contours and temperature along centerline comparisons with and without missile body.

two-dimensional, radially varying viscous profiles for the initial conditions at the nozzle exit plane location (calculated via two-dimensional kinetics) to define the starting boundary condition for the GIFS plume calculation. The final three-dimensional case (case 7) simulated the flowfield over the missile body, the base region, and the exhaust plume domains including the fuel-rich gas generator flow and chemical kinetics. Case 8 assumed a single equivalent nozzle approximation for the twin nozzle configuration. Cases 7 and 8 were initialized at the nozzle throat using a uniform inflow condition. The resulting two-dimensional profiles at the nozzle exit were comparable to the two-dimensional profiles used by case 6.

The following sections will discuss the individual influences of the various assumptions for phenomena simulated in the GIFS model.

Three-Dimensional Effect

In earlier studies,[2,12] it was shown that three-dimensional effects are significant and should not be ignored or oversimplified in modeling efforts. Figure 3 shows Mach contours for the three-dimensional solution. The plume expansion shock, barrel shock, and shock reflection are clearly visible downstream of the nozzle exit plane location. The static temperature is increased downstream of the reflection point, approaching a value slightly less than half the value of the total temperature of the flow. A comparison of the two-dimensional axisymmetric solution with the three-dimensional twin-nozzle solution was accomplished to determine the impact of the single equivalent nozzle assumption. Figure 4 provides a comparison of the axisymmetric and the three-dimensional solutions. There are significant differences between the two solutions, including the plume size, asymmetric flow distributions, and the location of the shock reflection points. Although these differences may infer that the axisymmetric solutions are inaccurate, the two-dimensional assumptions do provide insight concerning overall gross qualitative assessments, such as similarities in the barrel shock features and the global far-field properties. For parametric studies, axisymmetric simulations are often dictated as a result of time and computer resource constraints, but for detailed studies requiring accurate spatial resolution of multinozzle flows or flows with angle of attack, three-dimensional calculations are required.

Turbulence Effect

To assess the influence of turbulence in the plume flowfield solution resulting from twin nozzles, two three-dimensional calculations were performed, one assuming turbulent flow and the other assuming laminar flow. As would be expected, comparisons of flowfield results for turbulent and laminar cases, shown in Fig. 5, indicate decreasing trends in plume impingement intensity and plume mixing rate for the laminar calculation.

The comparison of static pressure contours in the horizontal and vertical plane is shown in Fig. 5. The turbulent and the laminar solutions are displayed in the same plot and are separated by $Z = 0$ line. Static temperature centerline axial profiles contrasting the turbulent and laminar solutions are shown in Fig. 6. These results indicate that the barrel shock reflection point is located approximately 8 m farther downstream for the turbulent solution. Therefore, the spatial characteristics of the plume flowfield, and hence, the location of the radiation centroid, can be influenced by the viscous stress model. The influence of different turbulence models was not assessed. The k-ε two-equation turbulence model[11] was applied exclusively in this study. In the present case at 47.6 km altitude, the effect of turbulence is not particularly strong. However, at lower altitudes, and hence, higher Reynolds numbers, turbulent effects will be more significant.

Internozzle Geometric Spacing Effect

The distance between the nozzles influences the location and strength of the plume/plume interactions. To explore this effect, perfect-gas, three-dimensional calculations were obtained at two different internozzle geometric spacings (narrow vs wide spacing). The variation in the distance between nozzle centerline locations for the two cases was ~15% with the first case assuming the widest separation distance. Figure 7 compares static temperature contours from the two solutions. These results indicate that internozzle spacing has a noticeable influence on the flowfield structure. As seen in Fig. 7, the initial plume expansion angle is larger for the wider spacing case, and the shock reflection location is farther downstream. A centerline axial profile of static temperature is displayed in Fig. 8, contrasting the two nozzle spacing solutions. The difference in the location of the shock reflection point is evident. Figure 8 also confirms that the increased static temperature of the wide spacing case extends throughout the calculation domain. It is concluded that the internozzle spacing affects the plume impingement shock location, the inviscid shock structure, and the shear-layer development. Thus, relatively small differences in internozzle spacing can impact the flowfield and it is likely to influence the plume radiative emissions.

Reacting Flow Effect

A frozen-chemistry solution was contrasted with a finite rate reacting solution to assess the significance of chemistry in complex plume flowfields. A comparison of the two calculations indicates that kinetic chemistry can effect the overall plume structure. Figure 9 is a centerline axial profile of static temperature extending from the nozzle exit plane to 150 m downstream. This comparison indicates that the chemistry model has an effect on the location of the barrel shock reflection point. The barrel shock reflection from the plume centerline occurs farther upstream for the reacting flow solution compared with the frozen case. However, overall, the comparison between the reacting and the frozen cases indicates that chemistry effects are not as significant at this high altitude condition. At high altitudes, the oxygen content of the ambient air is reduced and the ambient temperature and pressure are low. These conditions are not conducive to shear-layer combustion. It is expected that the chemistry effect will be more significant at lower altitudes, where plume/atmospheric afterburning will dominate the flowfield.

Nozzle Exit Boundary Condition Profile Effect

In a previous study,[5] to assess phenomena affecting scramjet nozzle performance, it was determined that performance is sensitive to variations in the radial profiles assumed for the start-line conditions. Thus, the influence of nozzle exit plane profile variations, assumed as starting conditions for the GIFS plume simulation, on the plume flowfield was investigated. In one case, radially varying nozzle exit plane profiles were determined via the TDK code. In the second case, uniform (one-dimensional) nozzle exit plane profiles were assumed. The uniform conditions had the same mass, energy, and momentum as the radially varying conditions. Plume expansions were then calculated for each case assuming fully turbulent, chemically reacting flow. Radial profiles of static temperature for both startline assumptions are shown at axial positions equal to 3, 10, and 20 m downstream of the nozzle exit in Fig. 10. A comparison of the spatial plume size indicates that the uniform start line results in a slightly larger radial plume-expansion because of the increased pressure difference between the nozzle exit and the freestream. As expected, differences between the two start-line approximations become less significant as the flow progresses axially downstream. Although these two solutions do not show a significant effect of exit profile shape on the plume temperature, it is expected that in other cases, particularly those with strong afterburning, differences in the shear stress between the core flow and the ambient airstream could affect the mixing rates, and consequently, the combustion chemistry in the shear layer. It should also be pointed out that the aforementioned solutions were obtained assuming a constant oxidizer/fuel (O/F) ratio across the inflow plane. When real engine effects such as fuel-film cooling and injector imperfections are accounted for, O/F can vary widely across the nozzle exit plane. To properly account for the effect of mixture ratio variations on the plume flowfield and the resulting base heat transfer effects, radially varying oxidizer-to-fuel ratios should also be considered.

Missile Body Effect

To assess the influence of the missile body and base region on the plume flowfield solution, a three-dimensional calculation was performed simulating the flowfield over the missile body, the base region, and the exhaust plume domain. This calculation also included the gas generator effluent. Figure 11a is static pressure in the missile base regions resulting from the nose-to-tail, three-dimensional solutions. Figures 11b and 11c are close-up views of Mach number vectors and static temperature contours, respectively, in the missile base flow region. The heating of the missile base surface and the effect of the gas generator effluent impinging on the nozzle surfaces are clearly evident. Further, the gas generator flow initially expands as it exits the nozzle, adjusting to the ambient pressure condition, but further downstream in the region between the two nozzles, the gas generator flow is compressed because of the area change created by the nozzle expansion skirt hardware. In Fig. 11b, showing the Mach vectors, the interaction of the gas generator flow with base regions and the nozzles is apparent. This interaction creates recirculation of the hot gases into the missile base region, evident in Fig. 11c. The blunt body shock, plume expansion shock, and shock reflection and resulting recirculation region are evident. Figure 12 contrasts static temperature contours and centerline static temperature profiles with and without the missile body included in the solutions. These results indicate that the plume expansion angles are larger and the overall plume width is wider if the missile body and base region are included in the computational domain. The expansion shock reflection point on the plume centerline is located 12 m farther downstream in the solution including the body and base. It appears that the missile body effects are significant and influences the inviscid shock structure, including the location of the reflection of the plume expansion shock and the plume shear-layer development.

Conclusions

A modified three-dimensional GIFS model was applied extensively for this study, which included seven different three-dimensional solutions and an axisymmetric approximation of the three-dimensional geometry. The effects of nozzle exit plane nonuniformity, internozzle spacing, turbulence, finite rate chemistry, and three-dimensional geometry were evaluated for a twin nozzle/plume propulsion configuration at a high altitude flight condition. Analysis of the solutions isolating these various effects leads to the following conclusions:

1) Start-line assumptions, two-dimensional radially varying vs one dimensional, uniform, had a significant effect on the immediate plume near-field calculation. The differences between the solutions resulting from the varying start-line assumption became less significant as the axial distance downstream of the nozzle exit plane increased. This significance of this sensitivity needs additional investigation to elucidate the effect of the starting conditions on the plume flowfield, particularly in the presence of strong afterburning and missile body/base flowfield interactions.

2) Comparison of solutions contrasting laminar flow and turbulent flow indicates that plume flowfield simulations are influenced by turbulence. Laminar flow approximations will degrade further at lower altitudes where turbulent mixing becomes more dominant.

3) The chemistry assumption (frozen vs reacting) did not significantly influence the overall plume structure in this high-altitude simulation. Some minor differences were noted; however, at the high-altitude flight condition simulated, chemistry effects are not dominant because the low pressure, cold temperature, and low atmospheric oxygen content of the ambient air are not conducive to shear-layer combustion. At lower-altitude conditions where the atmospheric oxygen content, ambient pressure and temperature are greater and shear-layer afterburning occurs, the chemistry effect may be significant.

4) The internozzle spacing distance has a significant impact on the barrel shock reflection location, plume/plume impingement shock location and shear layer. Instances where these influences may impact flowfield predictions occur when nozzle gimballing activities are considered.

5) A comparison of the two- and three-dimensional solutions indicates that the three-dimensional effects are important in the near-field plume and diminish as the axial distance extends farther downstream from the nozzle exit plane location. The single-equivalent-nozzle approach should not be used to describe plume near-field flow characteristics where three-dimensional plume impingement effects are dominant, and in the instances where three-dimensional spatial features are required as part of the flowfield description. In all cases, the single equivalent nozzle assumption should be carefully scrutinized. In some applications, the single equivalent nozzle assumption could be entirely inappropriate.

6) The missile body, base, and gas generator flow has a significant impact on the barrel-shock-reflection location, plume/plume impingement shock location, development of the shear-layer region, and the plume radial extent.

7) These analyses indicate that two-dimensional nonequilibrium analysis tools can provide some insight concerning overall gross

qualitative assessments of multiple plume flowfield phenomena. However, for detailed studies of complex flowfield phenomena, a more sophisticated three-dimensional calculation is required.

This study is intended to assess, understand, and demonstrate the significance of plume physical phenomena. This insight can be applied to develop engineering application analysis tools and identify where simplified models can be applied without compromising the validity of the solution results or the conclusions that might be deduced from analysis of the flowfield simulation.

Acknowledgments

Special gratitude is extended to Martha A. Simmons for her technical support, valuable insight, and assistance in preparing this paper.

References

[1]Shannan, R. V., and Murray, A., "Development of the KIVA-II CFD Code for Rocket Propulsion Applications," 10th Workshop for CFD Applications in Rocket Propulsion, NASA CP 3163, NASA Marshall Space Flight Center, April 1992.

[2]Ebrahimi, H. B., "Numerical Investigation on Multi-Plume Rocket Phenomenology," AIAA Paper 97-2942, July 1997.

[3]Dash, S. M., and Thorpe, R. D., "Shock Capturing Model for One and Two-Phase Supersonic Exhaust Flow," *AIAA Journal*, Vol. 19, No. 7, 1981, pp. 842–851.

[4]Dash, S. M., Wolf, D. E., Beddini, R. A., and Pergament, H. S., "Analysis of Two-Phase Flow Processes in Rocket Exhaust Plumes," *Journal of Spacecraft and Rockets*, Vol. 22, No. 3, 1985, pp. 367–380.

[5]Ebrahimi, H. B., "Parametric Investigation of the Effect of Various Phenomena on the Performance of a Scramjet Nozzle," AIAA Paper 95-6048, April 1995.

[6]Holcomb, J. E., "Development of an Adaptive Grid Navier–Stokes Analysis Method for Rocket Base Flows," AIAA Paper 88-2905, July 1988.

[7]Van Leer, B., "Flux-Vector Splitting for the Euler Equations," *Physics*, Vol. 170, Springer–Verlag, New York, 1982.

[8]Ebrahimi, H. B., "Validation Database for Propulsion Computational Fluid Dynamics," *Journal of Spacecraft and Rockets*, Vol. 34, Oct. 1997, pp. 642–650.

[9]Nickerson, G. R., "Two-Dimensional Kinetics (TDK) Nozzle Performance Computer Program," NAS8-36863, March 1989.

[10]"Titan II SLV Propulsion Subsystem," Gencorp, Aerojet Propulsion Div., Sacramento, CA, 1992.

[11]Jones, W. P., and Launder, B. E., "The Prediction of Laminarization with a Two-Equation Model of Turbulence," *International Developments in Heat Transfer*, Vol. 15, 1972, 303–314.

[12]Wrisdale, I. E., Mikulskis, D. F., and Gilmore, M. R., "Navier–Stokes Calculations of a Twin Nozzle Rocket Plume," AIAA Paper 96-1881, June 1996.

Color reproductions courtesy of Sverdrup Technology, Inc.